

The effect of rotation and viscous heating on the interpretation of experimental heat diffusivities in the edge pedestal

Weston M. Stacey

Fusion Research Center, Georgia Institute of Technology, Atlanta, Georgia 30332, USA

(Received 8 February 2010; accepted 8 April 2010; published online 17 May 2010)

A formalism is presented for evaluating the effect of plasma rotation, via viscous heating, on the interpretation of thermal conductivities from measured temperature and density gradients in the edge pedestal. An application to a H-mode DIII-D [J. Luxon, *Nucl. Fusion* **42**, 614 (2002)] discharge indicates that the effect could be significant. © 2010 American Institute of Physics.
[doi:10.1063/1.3422552]

I. INTRODUCTION

Understanding experimental thermal energy transport in the edge pedestal of tokamak H-mode plasmas has for several years been a major topic of plasma physics research. Two general approaches have been taken. The first approach is to attempt to match measured temperature and density profiles with transport code calculations by adjusting empirical transport coefficients (e.g., Ref. 1) or using theoretical transport coefficients (e.g., Ref. 2). The second approach is to invoke the heat conduction relation to infer the experimental heat diffusivity from measured temperature profiles using (e.g., Refs. 3–5). In principle, the total (heat+kinetic) “radial” energy flux, $Q_{\psi j}^{\text{exp}}$, can be determined from an experimental energy balance (e.g., Ref. 4), and the radial conductive heat flux, $q_{\psi j}^{\text{exp}}$, can then be determined by subtracting the convective heat, the inertial energy, and the viscous energy radial fluxes. In practice, the inertial and viscous energy flux corrections are always neglected, and the convective heat flux is sometimes neglected, as well.

Rather large and poloidally asymmetric flows have been measured in the scrape-off layers of tokamaks^{6,7} and predicted theoretically.^{6,8} While these flows are probably driven by drifts and other divertor and scrape-off layer phenomena, it stands to reason that flows in the SOL (scrape-off layer) will couple viscously across the separatrix to drive poloidally varying flows in the edge plasma. In fact, the very existence of the measured edge plasma flows in experiments with no external torque input would seem to demonstrate the existence of an inward torque transfer mechanism. Thus, it seems reasonable to expect that such poloidally asymmetric flows would also exist in the edge pedestal,⁹ implying the existence of significant rotational energy in the edge pedestal. This raises the question of the magnitude of viscous energy fluxes and viscous heating (conversion of rotational to thermal energy) in the edge pedestal and whether or not they need to be taken into account in the interpretation of heat diffusivities in the edge pedestal.

The purpose of this paper is to investigate the effect of edge plasma rotation, acting primarily through the work done by the plasma in flowing against the viscous stress, commonly known as “viscous heating,” on the determination of the conductive radial heat flux that should be used for the

interpretation of the experimental heat diffusivities from measured temperature and density profiles. The theoretical formulation is given in the next section, then applied to the interpretation of data from a DIII-D (Ref. 10) H-mode plasma shot in Sec. III. The results are summarized in Sec. IV.

II. THEORETICAL BACKGROUND

The heat conduction relation $q_{\text{cond}} = -n\chi dT/dr$ is used to infer the experimental heat diffusivity from measured temperature profiles using $\chi_j^{\text{exp}} = q_{\text{cond}}^{\text{exp}} L_T^{\text{exp}} / n^{\text{exp}} T^{\text{exp}}$. The total “radial” energy flux, $Q_{\psi j}^{\text{exp}}$, can be determined from an experimental energy balance,⁴ and the radial conductive heat flux, $q_{\psi j}^{\text{exp}}$, can then be determined by subtracting the convective, inertial, and viscous radial energy fluxes

$$q_{\psi j}^{\text{exp}} = Q_{\psi j}^{\text{exp}} - \left(\frac{5}{2} T_j + \frac{1}{2} m_j V_j^2 \right) n_j V_{\psi j} - Q_{\psi j}^{\text{II}}, \quad (1)$$

where

$$Q_{\psi j}^{\text{II}} = V_{\psi j} \Pi_{\psi \psi j} + V_{\theta j} \Pi_{\theta \psi j} + V_{\phi j} \Pi_{\phi \psi j} \quad (2)$$

is the radial viscous energy flux and the Π_{xyj} are the viscous fluxes of x -momentum in the y -direction. It is standard practice to neglect both the inertial and viscous radial energy flux corrections, and sometimes also to neglect the convective heat flux correction, in interpreting edge plasma heat diffusivities from experimental data.

Using the Braginskii viscosity formalism extended to orthogonal toroidal flux surface (ψ, p, ϕ) geometry,^{11,12} the radial viscous energy flux can be written to leading order as

$$\begin{aligned} Q_{\psi j}^{\text{II}} = & 2 \left[\eta_{0j} V_{\psi j} \left(\frac{1}{3} V_{pj} - f_p V_{\phi j} \right) + \eta_{4j} \left(V_{\phi j}^2 + \frac{1}{2} V_{\phi j} V_{pj} \right) \right] \\ & \times \left(\frac{1}{R} \frac{\partial R}{\partial l_p} \right) - \left(\frac{1}{3} \eta_{0j} V_{\psi j} + \frac{1}{2} \eta_{4j} V_{pj} \right) \left(\frac{\partial V_{pj}}{\partial l_p} \right) \\ & + (\eta_{0j} V_{\psi j} f_p - \eta_{4j} V_{\phi j}) \left[\frac{1}{R} \frac{\partial (R V_{\phi j})}{\partial l_p} \right] \\ & + \left(\frac{1}{3} \eta_{0j} V_{\psi j} V_{pj} - \frac{1}{2} \eta_{4j} V_{pj}^2 \right) \left[\frac{1}{R B_p} \frac{\partial (R B_p)}{\partial l_p} \right], \quad (3) \end{aligned}$$

where $f_p = B_\theta / B_\phi$ and the η_0 and η_4 are Braginskii’s parallel

and gyroviscosity coefficients, respectively, the first of which has been extended to the banana-plateau regime

$$\eta_{0j} = \frac{n_j m_j V_{thj} q R \varepsilon^{-3/2} \nu_j^*}{(1 + \varepsilon^{-3/2} \nu_j^*)(1 + \nu_j^*)}, \quad \eta_{4j} = \frac{n_j T_j}{\Omega_j}, \quad (4)$$

where $\Omega_j = Z_j e B / m_j$ is the gyrofrequency. Equation (3) explicitly displays the dependence of the viscous heating (energy flux) on the poloidal dependence of the flux surface parameters R and B_p and on the poloidal dependence of the toroidal and poloidal rotation velocities.

The poloidal ($p \approx \theta$) and toroidal velocities are measured (for carbon), and the radial ($\psi \approx r$) particle velocity can be determined from experimental particle balance. Evaluation of the above expression for $Q_{\psi j}^{\Pi}$ requires, in addition to these measurements of the carbon rotation velocities, models for the calculation of the deuterium rotation velocities,^{13,14} models for the poloidal variation in the flux surface quantities R and (RB_p) , and for the poloidal dependence of the toroidal rotation frequency (RV_ϕ) and the poloidal velocity. For the simple toroidal circular flux surface approximation $R(r, \theta) = R_0 + r \cos \theta$, $B_p = B_p^0 / (1 + (r/R_0) \cos \theta)$ the first term in $Q_{\psi j}^{\Pi}$ can readily be evaluated, the last term vanishes, and

$$\begin{aligned} RB_p &= R |\nabla \phi \times \nabla \psi| = \frac{\partial \psi}{\partial r} |\nabla r| = \frac{\partial \psi}{\partial r} \kappa^{-1} \Lambda(r, \theta) \\ &\equiv \frac{\frac{\partial \psi}{\partial r} \kappa^{-1} [\sin^2(\theta + x \sin \theta) (1 + x \cos \theta)^2 + \kappa^2 \cos^2 \theta]^{1/2}}{\cos(x \sin \theta) + \frac{\partial R_0}{\partial r} \cos \theta + [s_\kappa - s_\delta \cos \theta + (1 + s_\kappa) x \cos \theta] \sin \theta \sin(\theta + x \sin \theta)}, \end{aligned} \quad (7)$$

where

$$\frac{\partial \psi(r)}{\partial r} = \frac{|B_{\phi 0}| \kappa(r)}{2 \pi q(r)} \oint \left[\frac{d\ell_\theta}{1 + \frac{r}{R_0(r)} \cos(\theta + x \sin \theta)} \right] \Lambda(r, \theta). \quad (8)$$

Implementation of the Miller equilibrium model to derive an expression for the viscous energy flux will be carried out in a future investigation.

III. INTERPRETATION OF EDGE PEDESTAL HEAT DIFFUSIVITY IN A DIII-D H-MODE DISCHARGE

An ELMing H-mode, lower single null DIII-D discharge (#98889: $I = 1.2$ MA, $B = 2.0$ T, $P_{\text{nb}} = 3.1$ MW, $n = 4 \times 10^{19}/\text{m}^3$) that is being analyzed in some detail⁵ was selected. Data were averaged over the same subinterval (80%–99%) between ELMs (edge localized modes) for several successive ELMs in order to minimize the effect of random errors. Fits of the measured electron density and electron and ion temperature profiles are shown in Fig. 1. Fits of the mea-

the poloidal variation in (RV_ϕ) must be calculated. Here the angle θ is measured counterclockwise from the outboard midplane.

Making a Fourier expansion $V(r, \theta) \approx V^0(r)(1 + V^s \sin \theta + V^c \cos \theta)$ for both the poloidal and toroidal velocities leads to the following expression for the flux-surface average of Eq. (3)

$$\begin{aligned} \langle Q_{\psi j}^{\Pi} \rangle &\approx \frac{1}{R_0} \left\{ V_{\phi j}^0 V_{\phi j}^s \left[\eta_{0j} f_p V_{\psi j}^0 - \eta_{4j} \left(2V_{\phi j}^0 + \frac{1}{2} V_{p j}^0 \right) \right] \right. \\ &\quad \left. - \frac{1}{2} V_{p j}^0 V_{p j}^s \left[\eta_{0j} V_{\psi j}^0 + \eta_{4j} \left(V_{\phi j}^0 + \frac{1}{2} V_{p j}^0 \right) \right] \right\}. \end{aligned} \quad (5)$$

Equation (5) explicitly shows the dependence of the viscous energy flux on the up-down asymmetry in the rotation velocities.

A more accurate representation of the important poloidal dependence of the flux surfaces can be constructed from the Miller equilibrium model,¹⁵

$$\begin{aligned} R(r) &= R_0(r) + r \cos(\theta + x \sin \theta) \\ &\equiv R_0(r) + r \cos \xi \quad \text{where } x \equiv \sin^{-1} \delta \end{aligned} \quad (6)$$

and

measured carbon poloidal and toroidal rotation velocities are shown in Fig. 2. These measurements are obtained from a system of interleaved vertically viewing and toroidally viewing chords of the CER system. The measurements and data analysis are discussed in detail for the density and temperatures in Ref. 16 and for the rotation velocities in Refs. 17 and 18.

Also shown in Fig. 2 are calculated deuterium rotation velocities. The deuterium toroidal velocity was calculated by first using the measured carbon toroidal velocity to infer an experimental angular momentum transfer rate (Eqs. 12 and 14 of Ref. 17), then solving the deuterium toroidal momentum balance equation for the deuterium toroidal velocity (Eq. 13 of Ref. 17), using this inferred momentum transfer rate (to represent viscous and atomic physics momentum losses) and the measured carbon toroidal rotation. The deuterium poloidal rotation was calculated from poloidal momentum balance, using the measured carbon poloidal rotation and the parallel viscosity given by Eq. (14) of Ref. 14; i.e., using Eq. (25) of Ref. 14.

The flux surface averaged ion total radial energy flux

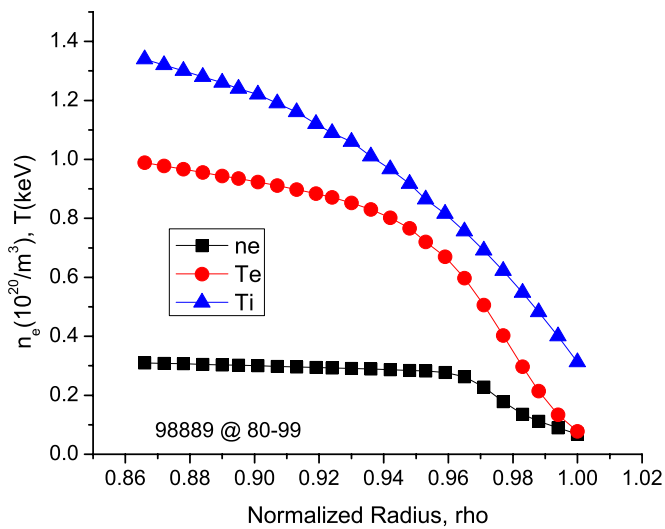


FIG. 1. (Color online) Experimental density and temperatures.

profile in the edge pedestal was calculated, following Ref. 4, by integrating the ion and electron energy balance equations inward from the separatrix, taking into account atomic physics and radiation losses, beam heating, ion-electron equilibration, neutral beam heating, etc., and using the experimentally determined value for the heat flux crossing the separatrix. The measured density and temperature profiles of Fig. 1 were used to evaluate these energy balance equations. Neutral atom recycling was calculated using a two-dimensional model of the edge region and divertor. The radial energy flux calculated in this way is shown as “total” in Fig. 3. The radial particle flux $\Gamma_{\psi j}$ was calculated using experimental measurements, the known beam particle source, and the calculated recycling neutral ionization source to evaluate the continuity equation, then $\Gamma_{\psi j}$ was multiplied by $2.5T_j^{\text{exp}}$ to obtain the quantity denoted “convective” and was multiplied by $0.5m_j(V_{\phi j}^2 + V_{\theta j}^2)$ to obtain the quantity denoted by “inertial.”

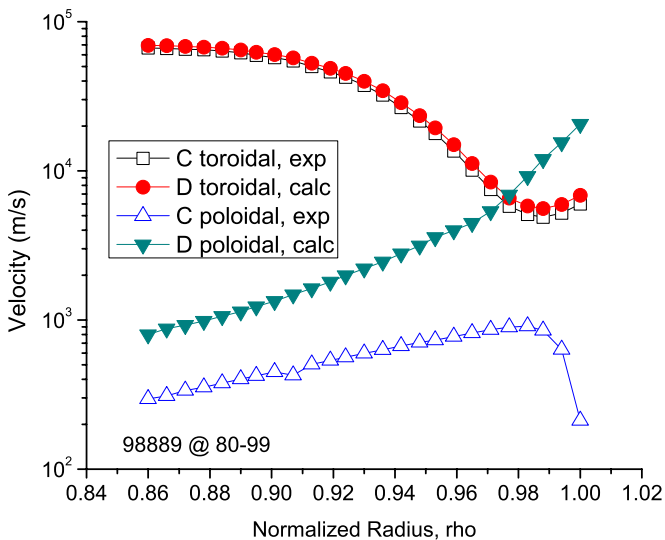


FIG. 2. (Color online) Experimental rotation velocities.

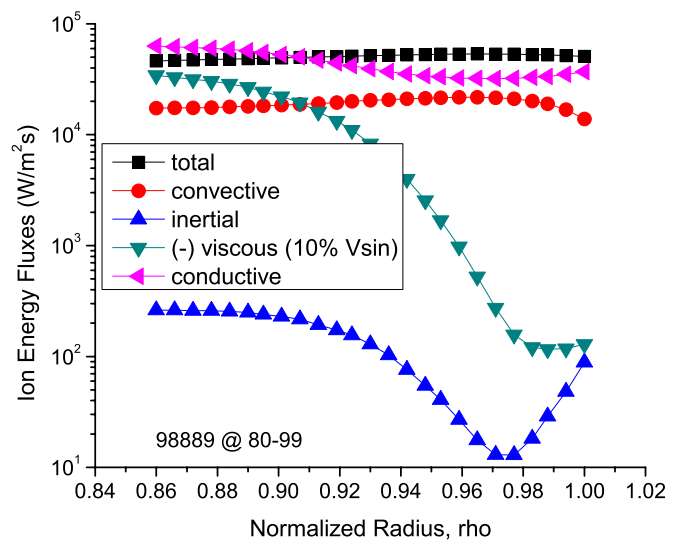


FIG. 3. (Color online) Calculated energy fluxes.

The profile denoted “viscous” was obtained by using the experimental data to evaluate Eq. (5), then multiplying by -1 for plotting purposes. Note that evaluation of Eq. (5) requires the determination of $\sin \theta$ components of the rotation velocities. We have a model¹³ for doing this from poloidal momentum balance, but the present version of this model cannot take into account the strong (order unity) poloidal asymmetry of the edge pedestal flux surfaces nor calculate the strong poloidal asymmetry in the rotation velocities observed in experiment^{6,7} and calculated in the scrape-off layer.^{6,8} We expect this strong poloidally varying flow in the SOL to be coupled viscously across the separatrix to drive poloidally varying flows in the confined plasma edge. It seems plausible that the poloidal variation in the edge plasma flows could be of order 1%–10%, so we made calculations for assumed 1% and 10% up-down asymmetries ($V_{\theta}^s = V_{\phi}^s = 0.01$ and 0.1). The result shown in Fig. 3 is for the 10% asymmetry.

The values of the experimental heat diffusivity $\chi_j^{\text{exp}} = q_{\text{cond}}^{\text{exp}} / n^{\text{exp}} T^{\text{exp}}$ inferred using the different experimental energy fluxes shown in Fig. 3 are compared in Fig. 4. The curve labeled “total” just uses the total energy flux calculated from the energy balance equation. Subtracting the convective heat flux from the total energy flux results in a significantly lower inferred heat diffusivity. Subtracting the convective, inertial, and viscous fluxes to obtain a true conductive heat flux with which to evaluate the above algorithm for the inferred heat conductivity results in significantly different values—results are shown for 1% and 10% assumed up-down asymmetries in the rotation velocities. Note that the negative “viscous energy flux” is really a viscous heating of the plasma, which converts rotation energy into thermal energy that must be removed, so the conductive heat flux actually increases when the viscous heating is taken into account.

Given the magnetic configuration of the edge plasma, with an elongation of 1.8 and a lower single-null divertor, and given the calculations^{6,8} of a highly poloidal asymmetric flow pattern in the SOL, a 10% vertical asymmetry in the edge pedestal rotation velocities seems a reasonable possibil-

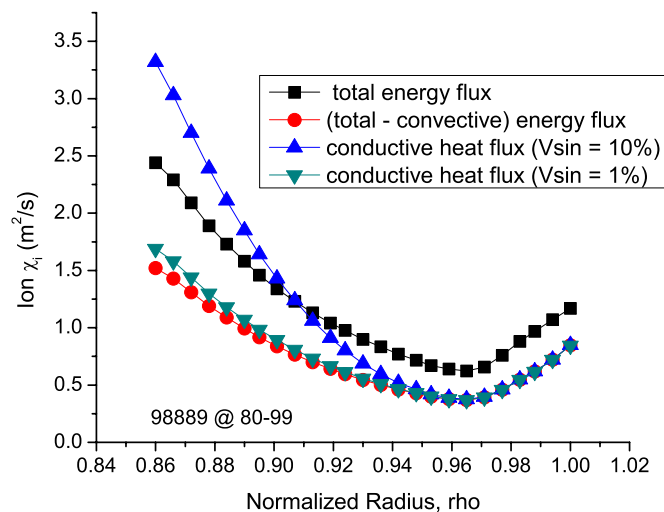


FIG. 4. (Color online) Inferred experimental thermal diffusivities.

ity. An asymmetry of this magnitude clearly would have a significant effect on the inferred heat diffusivities.

IV. SUMMARY AND CONCLUSIONS

A formalism has been developed for evaluating the viscous heating correction to the total ion radial energy flux in order to obtain the conductive heat flux, which should be used to interpret the thermal diffusivity from the measured density and temperature coefficients. An evaluation of the viscous heating correction in the edge pedestal of a DIII-D H-mode discharge, using measured rotation velocities and plausible 1%–10% up-down rotation velocity asymmetries, indicates that this correction to the inferred experimental thermal diffusivities could be significant. These results demonstrate the need to develop methods for the calculation and measurement of poloidal asymmetries in the toroidal and poloidal flow velocities in the edge plasma.

ACKNOWLEDGMENTS

The assistance of R. J. Groebner of General Atomics in analyzing and fitting the experimental data used in this paper is greatly appreciated.

This work was supported by the U.S. Department of Energy Grant No. DE-FG02-00-ER54538 with the Georgia Tech Research Corporation.

¹G. D. Porter, R. Isler, J. Boedo, and T. D. Rognlien, *Phys. Plasmas* **7**, 3663 (2000).

²T. Rafiq, A. Y. Pankin, G. Bateman, A. H. Kritz, and F. D. Halpern, *Phys. Plasmas* **16**, 032505 (2009).

³D. P. Coster, X. Bonnin, K. Borrass, H.-S. Bosch, B. Braams, H. Buerbaumer, A. Kallenbach, M. Kaufmann, J.-W. Kim, E. Kovaltsova, E. Mazzol, J. Neuhauser, D. Reiter, V. Rozhansky, R. Schneider, W. Ullrich, S. Voskoboinikov, P. Xantopoulos, and the ASDEX Upgrade Team, *Proceedings of the 18th Fusion Energy Conference*, Sorrento, Italy, 2000 (IAEA, Vienna, 2001).

⁴W. M. Stacey and R. J. Groebner, *Phys. Plasmas* **13**, 072510 (2006).

⁵J. A. Callen, R. J. Groebner, J. M. Canik, L. W. Owen, A. Y. Pankin, T. Rafiq, T. D. Rognlien, and W. M. Stacey, "Analysis of pedestal transport," *Nucl. Fusion* (submitted).

⁶M. Groth, G. D. Porter, J. A. Boedo, N. H. Brooks, R. C. Isler, W. P. West, B. D. Bray, M. E. Fenstermacher, R. J. Groebner, A. W. Leonard, R. A. Moyer, T. D. Rognlien, J. G. Watkins, and J. H. Yu, *J. Nucl. Mater.* **390–391**, 343 (2009).

⁷B. LaBombard, J. E. Rice, A. E. Hubbard, J. W. Hughes, M. Greenwald, F. S. Granetz, J. H. Irby, Y. Lin, B. Lipschultz, E. S. Marmor, K. Marr, D. Mossessian, R. Parker, W. Rowan, N. Smick, J. A. Snipes, J. L. Terry, S. M. Wolfe, S. J. Wukitch, and the Alcator C-MOD Team, *Phys. Plasmas* **12**, 056111 (2005).

⁸W. M. Stacey, *Phys. Plasmas* **16**, 042502 (2009).

⁹W. M. Stacey, *Phys. Plasmas* **16**, 062505 (2009).

¹⁰J. Luxon, *Nucl. Fusion* **42**, 614 (2002).

¹¹W. M. Stacey and D. J. Sigmar, *Phys. Fluids* **28**, 2800 (1985).

¹²W. M. Stacey and Cheonho Bae, *Phys. Plasmas* **16**, 082501 (2009).

¹³W. M. Stacey, R. W. Johnson, and J. Mandrekas, *Phys. Plasmas* **13**, 062508 (2006).

¹⁴W. M. Stacey, *Phys. Plasmas* **15**, 012501 (2008).

¹⁵R. L. Miller, M. S. Chu, J. M. Greene, Y. R. Lin-Liu, and R. E. Waltz, *Phys. Plasmas* **5**, 973 (1998).

¹⁶W. M. Stacey and R. J. Groebner, *Phys. Plasmas* **14**, 122504 (2007).

¹⁷W. M. Stacey and R. J. Groebner, *Phys. Plasmas* **15**, 012503 (2008).

¹⁸P. Gohill, K. H. Burrell, and R. J. Groebner, *Proceedings of the 14th Symposium on Fusion Engineering*, San Diego, 1991 (Institute of Electrical and Electronics Engineers, New York, 1992), Vol. 1, p. 1199.